# Experiments in Prompt γ-Ray Spectroscopy I NUCLEAR REACTION KINEMATICS

R. Collé<sup>1</sup>, H. M. Clark and I. L. Preiss

Department of Chemistry
Rensselaer Polytechnic Institute

Troy, New York 12181

Most laboratory courses teaching the skills of radiation detection, counting and spectroscopy utilize commercially available or in-house produced radionuclides which are brought to the counting facility. An important supplement to these courses would be laboratory experience in the techniques of on-line spectroscopy in which the detection and counting is done at the site of the nuclear reaction.

In as much as current nuclear chemistry research relies heavily on machine experiments, that is, those conducted on-line at the site of an accelerator or reactor, this can be a serious omission for the novice nuclear chemist who must encounter these experiences for the first time in his research. Unfortunately, very few schools have the facilities for teaching the methods of these experiments. The few available teaching accelerators are usually limited to physics or nuclear engineering programs. Although increasingly larger numbers of nuclear chemists eventually utilize research accelerators, essentially none of them are exposed to this on-line experience until they start their own research.

To whom all correspondence should be directed. Present address; Brookhaven National Laboratory, Department of Chemistry, Upton, Long Island, New York 11973

In contradistinction to the lack of teaching accelerators, many radiochemistry laboratories have available rather intense isotopic neutron sources (e.g.  $Po-\alpha-Be$  or  $Pu-\alpha-Be$ ). These sources have been used for a variety of experiments in which the activated samples are removed and counted off-site. These sources can also however be used with commonly available laboratory spectrometers to develop a number of interesting on-line experiments. In this and two future articles, a series of experiments in prompt  $\gamma$ -ray spectroscopy using a neutron source will be described. These experiments can be developed into a well-defined program which would be beneficial in introducing the student to this important aspect of experimental nuclear chemistry.

#### Nuclear Reaction Kinematics

A discussion of nuclear reaction kinematics is an integral part of every nuclear and radiochemistry course. This is certainly reflected in the treatment given in the most frequently used introductory texts (1-3) which devote from several pages to entire chapters on the subject. Its absence from the corresponding laboratory course is as assured as its presence in the theory or lecture course. Although many excellent experiments for accelerator teaching laboratories have been described (4-6), most require extensive instrumentation. The only frequently encountered kinematics experiment, using a neutron source, is the calculation of the neutron-proton mass difference from measurements of the  ${}^1{\rm H}(n,\gamma){}^2{\rm H}$  reaction  $\gamma$ -ray energy (6-8). The observation and measurement of the Doppler broadening of  ${}^1{\gamma}$ -rays from reactions is another simple, but instructive experiment. This can be

demonstrated with a single  $\gamma$ -ray spectrometer using the  $^9\text{Be}(\alpha,n\gamma)^{12}\text{C}$  reaction of the neutron source. A discussion and description of the experiment will be made here.

#### Reaction Doppler Broadening

The neutrons of isotopic sources are produced by  $(\alpha,n)$  reactions from a mixture of beryllium and an  $\alpha$ -emitter (e.g.  $^{23}$ Pu or  $^{210}$ Po). After an  $\alpha$ -particle is absorbed by a Be nucleus, the compound nucleus ( $^{13}$ C\*) is set in motion due to the initial kinetic energy of the  $\alpha$ -particle. Following neutron emission from the compound nucleus, the  $^{12}$ C\* product nucleus moves with a velocity due to both the compound nucleus velocity and the neutron emission recoil. This  $^{12}$ C\* nucleus is not necessarily produced in the ground state, but can be left in the 4439 keV first excited state. The de-excitation to the ground state is accompanied by a 4439 keV  $\gamma$ -ray. If the  $\gamma$ -ray transition occurs while the  $^{12}$ C\* nucleus is in motion it will be Doppler broadened depending on the velocity and relative angles of emission.

Let us develop the kinematics of this situation for a general case.  $^{3}$ 

Consider the non-relativistic collision of two particles,  $m_1$  with initial velocity  $v_1$ , and  $m_2$  at rest. By definition of the center of mass,

$$\mathbf{m}_{1}\overline{\mathbf{v}}_{1} = \mathbf{m}_{2}\overline{\mathbf{v}}_{2} \tag{1}$$

where  $\overline{v}_1$  and  $\overline{v}_2$  refer to the velocities of the two particles in the

<sup>&</sup>lt;sup>2</sup>This state is populated in  $(54 \pm 4)\%$  of the reactions for a Pu- $\alpha$ -Be neutron source, cf. Drake, et. al. (9).

<sup>&</sup>lt;sup>3</sup>A more complete treatment of the kinematics can be found in Michalowicz (10).

center of mass system (CM). The center of mass travels with velocity V in the laboratory coordinate system (LAB). Therefore,

$$\overline{v}_1 = v_1 - V \tag{2}$$

and

$$\bar{v}_2 = v \qquad . \tag{3}$$

Substitution of eqs. (2) and (3) into (1) and rearranging yields

$$v = \begin{bmatrix} \frac{m_1}{m_1 + m_2} \end{bmatrix} v_1 \qquad (4)$$

Thus,

$$\overline{v}_1 = v_1 - \left[ \frac{m_1}{m_1 + m_2} \right]$$

$$= \left\lceil \frac{m_2}{m_1 + m_2} \right\rceil v_1 \tag{5}$$

and

$$\overline{\mathbf{v}}_2 = \left[ \frac{\mathbf{m}_1}{\mathbf{m}_1 + \mathbf{m}_2} \right] \mathbf{v}_1 \qquad . \tag{6}$$

Since the kinetic energy T is given by

$$T = 1/2 \text{ mv}^2 = 1/2 \text{ M} \left[ \frac{v_2}{c_2} \right]$$
 (7)

where M is the energy equivalent of mass in MeV, the eqs. (5) and (6) may also be expressed in terms of energy.

$$\bar{T}_1 = \left[\frac{M_2}{M_1 + M_2}\right]^2 T_1$$
 (8)

$$\bar{T}_2 = \left[ \frac{M_1 M_2}{(M_1 + M_2)^2} \right] T_2 .$$
 (9)

The initial total kinetic energy of the system in CM is then just the sum of (8) and (9)

$$\bar{T} = \bar{T}_1 + \bar{T}_2 = \begin{bmatrix} \frac{M_2}{M_1 + M_2} \end{bmatrix} T_1$$
 (10)

The conservation of energy in the CM requires

$$1/2 \, M_3 \left[ \frac{\bar{v}_3}{c} \right]^2 + 1/2 \, M_4 \left[ \frac{\bar{v}_4}{c} \right]^2 = \bar{T} + Q - E_{ex} , \qquad (11)$$

where Q is the total reaction Q-value given by

$$Q = M_1 + M_2 - M_3 - M_4$$

$$= T_3 + T_4 - T_1$$
 (12)

and  $E_{ex}$  is the excitation energy of the state that the product  $M_4$  is left in. The term  $(Q - E_{ex})$  may be considered as an effective reaction Q-value. Imposing the definition of CM,

$$M_3 \bar{v}_3 = M_4 \bar{v}_4$$
 (13)

on eq. (11) and solving for  $(\overline{v}_{\underline{\iota}}/c)$  yields

$$\frac{\bar{v}_4}{c} = \sqrt{\frac{2 M_3(\bar{T} + Q - E_{ex})}{M_4(M_3 + M_4)}}$$
 (14)

Similarly,

$$\frac{\bar{v}_3}{c} = \sqrt{\frac{2 M_4 (\bar{T} + Q - E_{ex})}{M_3 (M_3 + M_4)}}$$
 (15)

From eq. (4) the velocity of the center of mass in the LAB can also be expressed as

$$\frac{v}{c} = \sqrt{\frac{2 M_1 T_1}{(M_1 + M_2)^2}}.$$
 (16)

The first order Doppler shift of a wave emitted (or absorbed) by a moving object is

$$\frac{\Delta v}{v} = \frac{v}{c} = \frac{\Delta E_{\gamma}}{E_{\gamma}} \qquad (17)$$

The maximum energy shift of an emitted  $\gamma$ -ray due to the motion of the center of mass in the LAB is

$$\Delta E_{\gamma} = (\frac{V}{c}) E_{\gamma}$$
 (18)

where (V/c) is given by eq. (16). The maximum energy shift due to the motion of  $\rm M_{\Delta}$  with respect to the CM is

$$\Delta E_{\gamma} = (\frac{\overline{V}_4}{c}) E_{\gamma} \tag{19}$$

where  $(\overline{v}_4/c)$  is given by eq. (14). The maximum and minimum broadening is therefore

$$(\Delta E_{\gamma})_{\text{max}} = (\frac{V}{c} + \frac{\overline{V}_{4}}{c})E_{\gamma}$$
 (20)

and

$$(\Delta E_{\gamma})_{\min} = (\frac{v}{c} - \frac{\overline{v}_4}{c})E_{\gamma}$$
 (21)

respectively. This broadening is illustrated in Figure 1. If a  $\gamma$ -ray of energy  $E_{\gamma}$  is emitted in the direction of the CM, it is energy shifted to  $E_{b}$ . If it is emitted at 180° to the CM direction, it is shifted to  $E_{a}$ . Depending on the relative angle of emission, the  $\gamma$ -ray can be shifted to any energy between  $E_{a}$  and  $E_{b}$ . Similarly, the direction of the  $\gamma$ -ray relative to the direction of  $M_{4}$  in the CM determines the maximum and minimum shift from the center of mass. For example, as shown in Figure 1, if the center of mass motion shifts the energy to  $E_{a}$ , the maximum and minimum broadening due to the motion of  $M_{4}$  from the center is  $E_{d}$  and  $E_{c}$ , respectively.

The maximum broadening will occur only if the  $\gamma$ -ray is emitted before the product nucleus  $M_4$  slows down. This is determined by the lifetime of the product nucleus excited state compared to the energy loss (slowing down) of ions in matter. If the excited state is sufficiently long-lived

that M<sub>4</sub> comes to rest, then broadening of the \gamma-ray will not occur. Schwarzchild and Warburton (11) have discussed the Doppler broadened lineshapes of \gamma-rays as a function of the energy losses and lifetimes. Unless both the lifetime and energy losses are well known, it is impossible to adequately calculate the broadening. Actually, in practice, measurements of the Doppler shift are used to determine short nuclear lifetimes (11).

# <sup>9</sup>Be(α,nγ)<sup>12</sup>C Reaction

In the isotopic neutron sources the orientation of the initial  $\alpha$ -particle direction and the Be nuclei is random. Therefore, the distribution of center of mass directions is isotropic and the energy shifts can take on any value between  $E_a$  and  $E_b$  of Figure 1. Similarly, since the neutron emission is isotropic, the  $^{12}\text{C*}$  product nucleus can recoil at any angle (0°-180°) to the center of mass direction. The maximum shift ( $E_f$  of Figure 1) occurs when the  $\gamma$ -ray is emitted in both the direction of the center of mass and the  $^{12}\text{C*}$  nucleus. The minimum shift ( $E_c$  of Figure 1) occurs with  $\gamma$ -emission at 180° to both directions. The total maximum broadening is therefore

$$\Delta E_{\gamma} = 2 \left( \frac{V}{c} + \frac{\overline{V}_4}{c} \right) E_{\gamma}$$
 (22)

where (V/c) and  $(\overline{v}_4/c)$  are given by eqs. (16) and (14), respectively.

For a  $^{239}$ Pu- $\alpha$ -Be source, using the data provided in Table I, the maximum broadening calculated from eqs. (16), (14) and (22) is

with 
$$\frac{\Delta E_{\gamma}}{c} = 216 \text{ keV}$$

$$(\frac{V}{c}) E_{\gamma} = 72 \text{ keV}$$
and 
$$(\frac{\overline{V}_{4}}{c}) E_{\gamma} = 36 \text{ keV}$$

This maximum broadening will be evidenced only under the ideal conditions of the calculation. The factors which inhibit the maximum broadening follow:

- a) The average incident  $\alpha$ -particle energy may be lower due to losses on interactions in the source.
- b) The 13C\* compound nucleus may slow down before neutron emission.
- c) The <sup>12</sup>C\* product nucleus may slow down before the γ-ray is emitted.
- d) The over-all reaction may not be isotropic due to inhomogenuity in the source.

#### Doppler Broadening Measurement

The line-shape of a Doppler broadened  $\gamma$ -ray with maximum broadening is very nearly rectangular. The origin of this shape is illustrated in Figure 2. Although each  $\gamma$ -ray is monoenergetic, it is detected with a finite line-width due mainly to the spectrometer resolution. If a  $\gamma$ -ray of energy  $E_{\gamma}$  and detection resolution of FWHM is Doppler broadened to energies between  $E_{c}$  and  $E_{f}$ , the detected line consists of a continuous spectrum of unresolved monoenergetic  $\gamma$ -rays each with a detection resolution of FWHM. The overlap of these  $\gamma$ -rays produced the observed result shown in Figure 2.

Observation and measurement of the Doppler broadening thus necessitates a spectrometer with a resolution much smaller than the broadening. Liquid nitrogen cooled Ge(Li) detectors adequately meet this requirement. For these detectors, the FWHM for a  $\gamma$ -ray peak at 4439 keV is only several keV. Unfortunately, the readily available NaI(Tl) scintillators are not however, since the FWHM is larger than the broadening.

The experiment essentially consists of making a comparison of the measured broadening to the maximum calculated Doppler width. Students should be expected to derive all the equations necessary for the calculation and to explain the observed line-shape. The crux of the experiment is not only to demonstrate reaction Doppler broadening, but also introduce students to the concept and process of observing reactions in progress.

The specific experimental details depend to a large extent on the instrumentation available. The ability to obtain a y-ray spectrum of the neutron source with an adequate resolution is all that is necessary. The spectrometer must be energy calibrated in the 4.4 MeV region and must also have a known detection resolution. The latter condition is to insure that Doppler broadening is observed and not just the detection resolution. A simple way to make the measurement and simultaneously calibrate the spectrometer is to obtain the spectrum with the source in a water moderator. A typical spectrum of a <sup>239</sup>Pu/Be source in water obtained with a Ge(Li) detector is shown in Figure 3. The peak at 2223 keV and its pair production escape peaks [2223-551 and 2223-2(511) keV] are due to thermal neutron capture in the hydrogen  $[{}^{1}H(n,\gamma)^{2}H]$  of the water. 4 It is the energy measurement of this transition which constitutes the experiment to determine the neutron-proton mass difference (6-8). The peak at 6129 keV and its escape peaks [6129-511 and 6129-2(511) keV] is from an  $^{16}$ O transition due to inelastic scattering of fast neutrons from oxygen  $[^{16}O(n,n'\gamma)^{16}O]$  of the water<sup>4</sup>. The  ${}^{9}$ Be( $\alpha$ ,n $\gamma$ )<sup>12</sup>C reaction Doppler broadened lines at 4439 keV

<sup>&</sup>lt;sup>4</sup>A more thorough discussion of the origin of these prompt γ-rays is provided in Parts II and II of this series.

(full energy peak), 4439-511 keV (single escape peak), and 4439-2(511) keV (double escape peak) are located between the two sets of lines from the  $^{1}$ H(n, $\gamma$ ) and  $^{16}$ O(n, n' $\gamma$ ) reactions. The known energies of these transitions can be used to establish an energy calibration line to locate the position and width of the  $^{9}$ Be( $\alpha$ ,n $\gamma$ ) Doppler broadened lines. The spectrum, as shown in Figure 3, also establishes the detection resolution at the 4439 keV line by interpolation from the two sets of unbroadened lines.

The specific details regarding the instrumentation and methodology for our measurement follow. It is intended only as an example since the experiment could be implemented with much less sophisticated instrumentation.

#### <u>Experimental</u>

The neutron source  $^5$  used consisted of an intimate mixture of 47.0 g  $^{239}$ Pu as  $^{239}$ Pu as

Singles  $\gamma$ -ray spectra were obtained with a liquid nitrogen cooled 30-cm $^3$  wrap-around coaxial Ge(Li) detector (Canberra Industries) coupled to a charge sensitive FET preamplifier. The pulses were routed through an

This source was fabricated by the Nuclear Sources Division of the Monsanto Research Corp. and obtained with an (?) grant.

Wisiflux Neutron Howitzer, Model 135, Reactor Experiments Inc., Belmont, Calif.

amplifier-biased amplifier system to select regions of interest and accumulated in either a 1024-channel pulse height analyzer or into 4096 channels of a two-dimensional 64 x 64 analyzer. Since the region of interest is 4-6 MeV wide, accurate measurements of spectral shapes and peak positions were made with the larger memory capacity (4096 channels), providing a dispersion of approximately 1-2 keV per channel. For routine measurements, the smaller memory (1024 channels) was used with a dispersion of at least 4 keV per channel. The over-all integral linearity of the spectrometer (detector, amplifiers, ADC and analyzer memory) was checked with a precision pulser (Geoscience Model 2010) using the method given by Crouch and Heath (16) and found to be linear to better than 0.1% over 100% of the analyzer memory.

For an initial set-up, the spectrometer is energy calibrated in the low energy region (< 2 MeV) using standard radioactive sources (e.g. <sup>137</sup>Cs, <sup>60</sup>Co and <sup>88</sup>Y). Pulser peaks are then superimposed on the spectrum and the pulser units converted into energy units. The pulser can then be used to locate any energy portion of the entire spectrum. A crude calibration can be made by using the very intense 4439 keV radiation from the source itself. The large broadening of these peaks do not allow accurate energy location, but they are extremely convenient for a rapid estimate of the correct region. Once the approximate energy region is located, the spectrum can be accurately calibrated using some well established transitions due to neutron interactions and by taking advantage of the known separation (511 keV) of the γ-ray pair production escape peaks. Two convenient transitions, as previously described, are the 2223 keV and 6129 keV from the

 $^{1}$ H(n, $\gamma$ ) and  $^{16}$ O(n, $^{\alpha}\gamma$ ) reactions. These transitions are easily detected by placing the neutron source in water. Other high energy  $\gamma$ -rays obtained from thermal neutron radiative capture could also be used (see footnote 3).

The detection resolution (FWHM) for the Ge(Li) spectrometer was measured as a function of energy from 120 to 7900 keV. The results are provided in Table II and figure 4. This was used to confirm that the  $^9{\rm Be}(\alpha,n\gamma)$   $\gamma$ -ray is indeed broadened beyond the detection resolution and also to obtain the resolution at 4439 keV. Detector resolution versus energy for other Ge(Li) configurations have been reported (18-20).

Once the spectrometer is accurately calibrated for energy and resolution, a spectrum of the neutron source in water is taken. Typical spectra are shown in Figure 3 and 5.

## Results and Discussion

To obtain the Doppler width, the observed line must be measured at or near the peak baseline. In this case, the total <u>FWHM</u> of the line is meaningless since the broad peak consists of a continuous series of lines and not a single line as in most γ-ray peaks. Two uncertainties must be considered when making the measurement. The first is the uncertainty in the exact location of the end of the line and the beginning of the baseline. The second involves the finite detection resolution at the ends of the broadened lines. A typical calculation on the full energy peak of Figure 5 follows:

Energy calibration = 1.79 keV/cm

line-width at base = 106 chs

uncertainty in base-width = 8 chs

FWHM (4.4 MeV) = 6.6 keV

WIDTH = 1.79(106) ± [1.78(8) + 2(6.6)] keV

= (190 ± 28) keV

The uncertainty in the line-width at the base was estimated to be eight channels (i.e. two channels in either direction at each end of the line) and the uncertainty in the detection resolution at the line ends was taken as twice the detection resolution (FWHM) at 4.4 MeV. The results of the calculation on the other peaks 7 of Figure 5 are provided in Table III.

The measured limits are within the calculated maximum value (216 keV) and one might conclude that maximum broadening occurs. This is not true since the observed line shape is not rectangular, but rather has started to collapse. That is to say, the <sup>12</sup>C\* product nucleus has started to slow down before the γ-ray was emitted. This slowing down would be first evidenced by the depletion (collapse) of the ends of the line. Interested students could pursue the matter further by discovering how the Doppler widths and line shapes change with the nuclear lifetimes for given reactions. A good source to start with is Schwarzchild and Warburton's review article (11). Lastly, more advanced students could utilize their measurement of the Doppler broadening of the γ-ray line to determine the lifetime of the 4439 keV <sup>12</sup>C excited state. The lifetime measurement by this method was originally made by Catz and Amiel (21), and a similar advanced laboratory experiment using their method has been described by Campbell, et. al. (22).

The widths of the escape peaks are, of course, further broadened to a small extent due to the Doppler broadening of the escaping annihilation radiation. This broadening is insignificant however, in comparison to that due to the recoiling 12C\* nucleus.

Literature Cited

(1) Friedlander, G., Kennedy, J. W., and Miller, J. M., "Nuclear and Radiochemistry", 2nd ed., John Wiley and Bons, Inc., New York, 1964.

is a considerable

Herts of there yes were we. Her with

and the Committy of the field good steels maying

- (2) Harvey, B. G., "Introduction to Nuclear Physics and Chemistry", 2nd ed., Prentice-Hall, Inc., Englewood Cliffs, New Jersey, 1969.
- (3) Halliday, D., "Introductory Nuclear Physica", 2nd ed., John Wiley and Sons, Inc., New York, 1953.
- (4) Duggan, J. L. (editor), "Proceedings of the Conference on the Use of Small Accelerators for Teaching and Research", Oak-Ridge,

  CONF-680411, TID-4500 (1968). Available from U. S. Dept. of Commerce,

  NBS, Clearinghouse for Federal Scientific and Technical Information,

  Springfield, Va. 22151. (Contains many useful references.)
- (5) "Applications of Small Accelerators", Proceedings of a Symposia, Amer.

  Nucl. Soc., BRH-CFS-70-2, PB-190-994 (1970). Available from U. S.

  Dept. of Commerce as listed in ref. (3). (Contains many useful references.)
- (6) Bygrave, W., Treado, P., and Lambert, J., "Accelerator Nuclear Physics:
  Fundamental Experiments with a Van de Graaff Accelerator", High Voltage
  Engineering, Burlington, Mass., 1971.
- (7) Overman, R. T., "Laboratory Manual A", Ortec, Inc., Oak Ridge, Tenn., 1968.
- (8) Banta, H. E. and Noakes, J. E., Amer. J. Phys. 35, 739 (1967).
- (9) Drake, D. M., Hopkins, J. C., et. al., Nucl. Instru. and Meth. 62, 349 (1968).
- (10) Michalowicz, A., "Kinematics of Nuclear Reactions", Iliffe Books, London, 1967.

- (11) Schwarzchild, A. Z. and Warburton, E. K., Ann. Rev. Nucl. Sci. 18, 265 (1968).
- (12) Lederer, E. M., Hollander, J. M. and Perlman, I., "Table of Isotopes", 6th ed., John Wiley and Sons, Inc., 1968, p. 432.
- (13) Marion, J. B., Nucl. Data A4, 301 (1968).
- (14) Maples, C., Goth, G. W. and Cerny, J., Nucl. Data A2, 429 (1966).
- (15) Wapstra, A. H. and Gove, N. B., Nucl. Data 9, 267 (1971).
- (16) Crouch, D. F. and Heath, R. L. in O'Kelley, G. D. (editor),

  "Application of Computers to Nuclear and Radiochemistry", National

  Academy of Sciences, Nuclear Science Series, NAS-NS-3107, 1962, p. 84.

  Available from U. S. Dept. of Commerce as listed in Ref. (3).
- (17) Bartholomew, G. A., Groshev, L. V., et. al., Nucl. Data 3, 538 (1967).
- (18) Cappellani, F. and Restelli, G. in Bertolini, G. and Coche, A. (editors), "Semiconductor Detectors", John Wiley and Sons, Inc., New York, 1968, p. 385.
- (19) Hague, A. K. M. M., Nucl. Instru. and Meth. 94, 349 (1971).
- (20) Cline, J. E. and Heath, R. L., "Gamma-Ray Spectrometry of Neutron Deficient Isotopes", Idaho Nuclear Corp., Ann. Prog. Rpt. IN-1130 (TID-4500), 1969, p. 7.
- (21) Catz, A. L. and Amiel, S., Nucl. Phys. A92, 222 (1967).
- (22) Campbell, J. L., O'Brien, P., and MacKenzia, I. K., Amer. J. Phys. 40, 9 (1972).

Table I

### Relevant Nuclear Data

a) <sup>239</sup>Pu average Eα (12):

5.157 MeV (73.3%)

5.145 MeV (15.1%)

5.107 MeV (11.5%)

5.15 MeV (average)

b)  $^{12}$ C E<sub>Y</sub> (13):

 $4.4390 \pm 0.0002 \text{ MeV}$ 

c) <sup>9</sup>Be(a,n) Q-value (14): .

5.7038 ± 0.0010 MeV

d) Mass Excesses (15):

n 8.07169 ± 0.00010 MeV <sup>4</sup>He 2.42494 ± 0.00025 MeV <sup>9</sup>Be 11.3484 ± 0.0006 MeV <sup>12</sup>C 0

1

Table II

Detection Resolution versus γ-Ray Energy

Source	E <sub>Y</sub> (keV) <sup>†</sup>	FWHM (keV)
57 <sub>Co</sub>	121.94 ± 0.05	2.8 ± 0.08
133 <sub>Ba</sub>	356.27 ± 0.14	3.0 ± 0.06
<sup>137</sup> Cs	661.635 ± 0.076	$3.1 \pm 0.06$
54 <sub>Mn</sub>	834.81 ± 0.03	3.2 ± 0.06
<sup>56</sup> Co	846.76 ± 0.05	3.1 ± 0.06
88 <sub>Y</sub>	898.04 ± 0.04	3.2 ± 0.06
<sup>60</sup> Co	1173.23 ± 0.04	3.5 ± 0.07
<sup>60</sup> co	$1332.49 \pm 0.04$	$3.6 \pm 0.07$
88 <sub>Y</sub>	1836.13 ± 0.04	4.0 ± 0.12
$\frac{1}{H(n,\gamma)}$	2223.29 ± 0.06	4.5 ± 0.14
<sup>56</sup> Co	2598.80 ± 0.12	4.8 ± 0.25
$^{16}$ 0(n,n $^{\dagger}$ Y)	6129.3 ± 0.4	8.4 ± 0.67
<sup>63</sup> Cu(n,γ)	7916 ± 1	11.1 ± 0.80

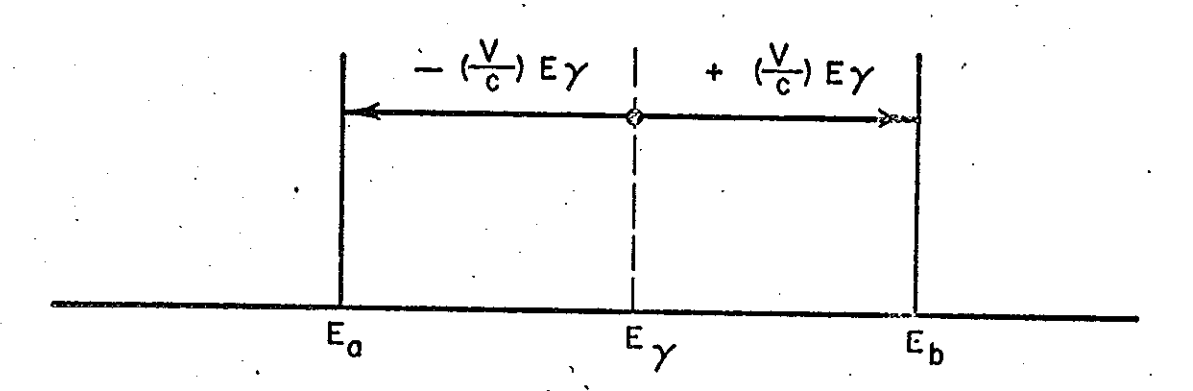
<sup>&</sup>lt;sup>†</sup>Values for  $E_{\gamma}$  taken from ref. (13), except that for <sup>57</sup>Co [ref. (12)] and <sup>63</sup>Cu(n, $\gamma$ ) [ref. (17)].

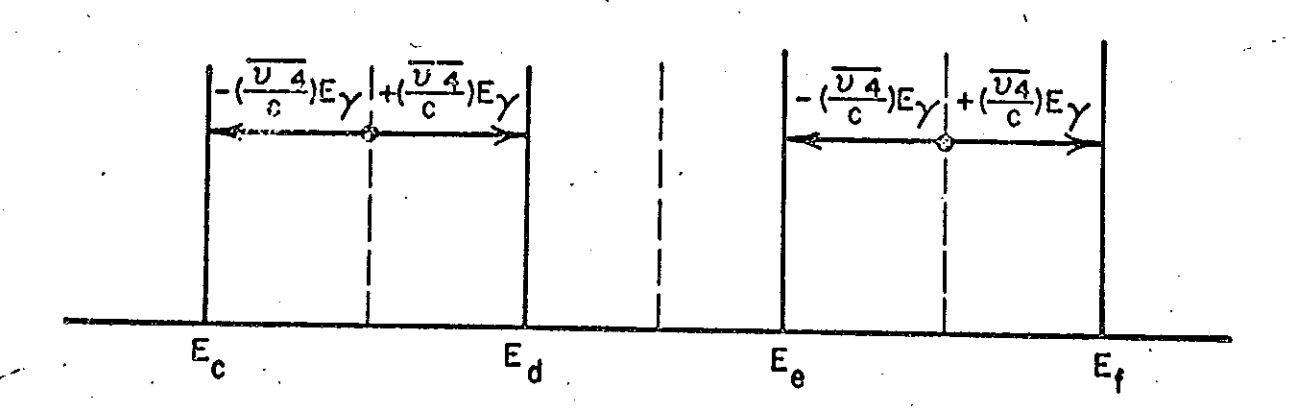
Table III Width of  $^9 \text{Be}(\alpha,n\gamma)$  4.439 MeV  $\gamma\text{-Ray}$ 

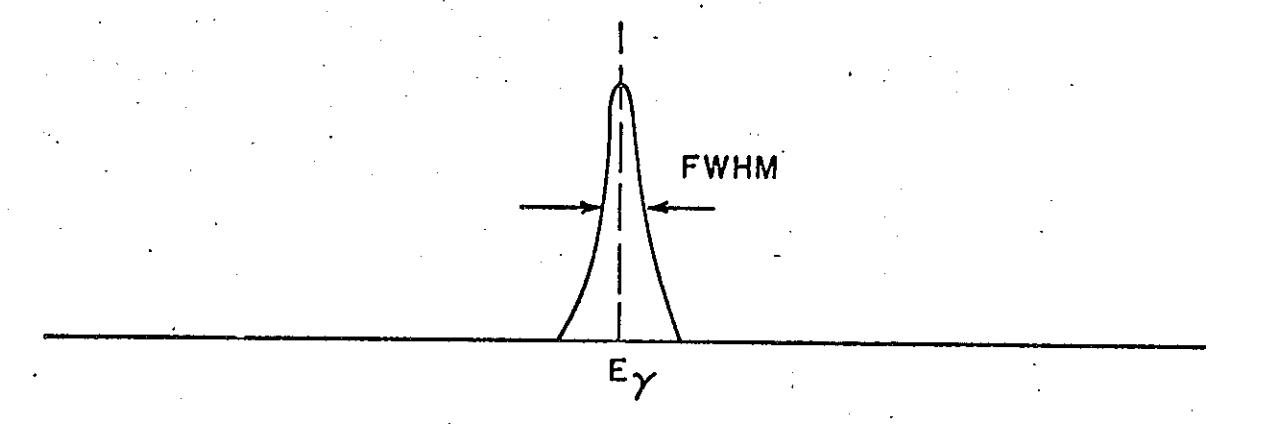
	Full Energy Peak	Single Escape Peak	Double Escape Peak
energy calibration	1.79 keV/ch	1,79 keV/ch	1.79 keV/ch
base width	106 chs	92 chs	120 chs
uncertainty in base width	8 chs	8 chs	8 chs
FWHM (4.4 MeV)	6.6 keV	<b>6.</b> 6 keV	6.6 keV
Width	_ 190 keV	<b>1</b> 65 keV	215 keV
uncertainty in width	28 keV	28 keV	28 ke <b>V</b>
average width		190 ± 28 keV	•

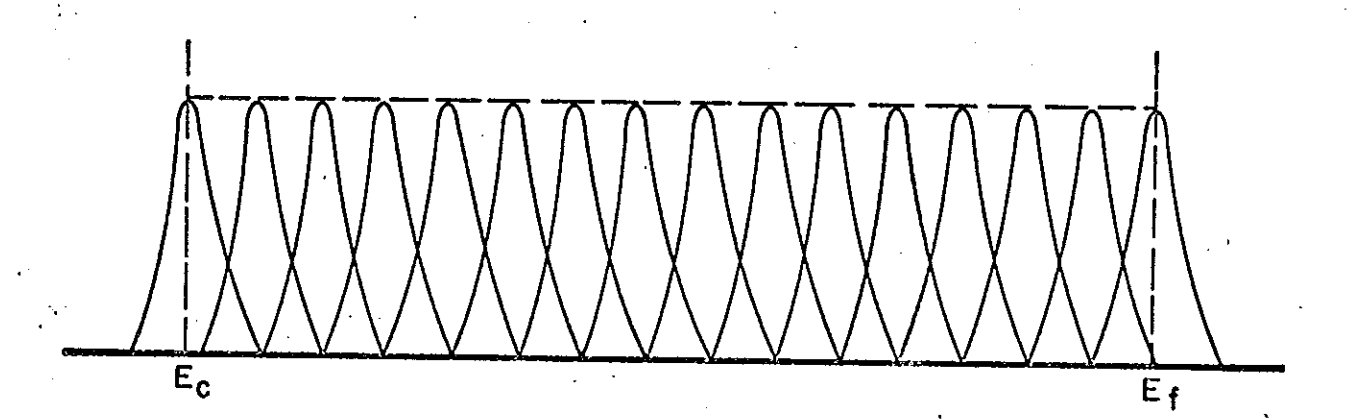
#### Figure Captions

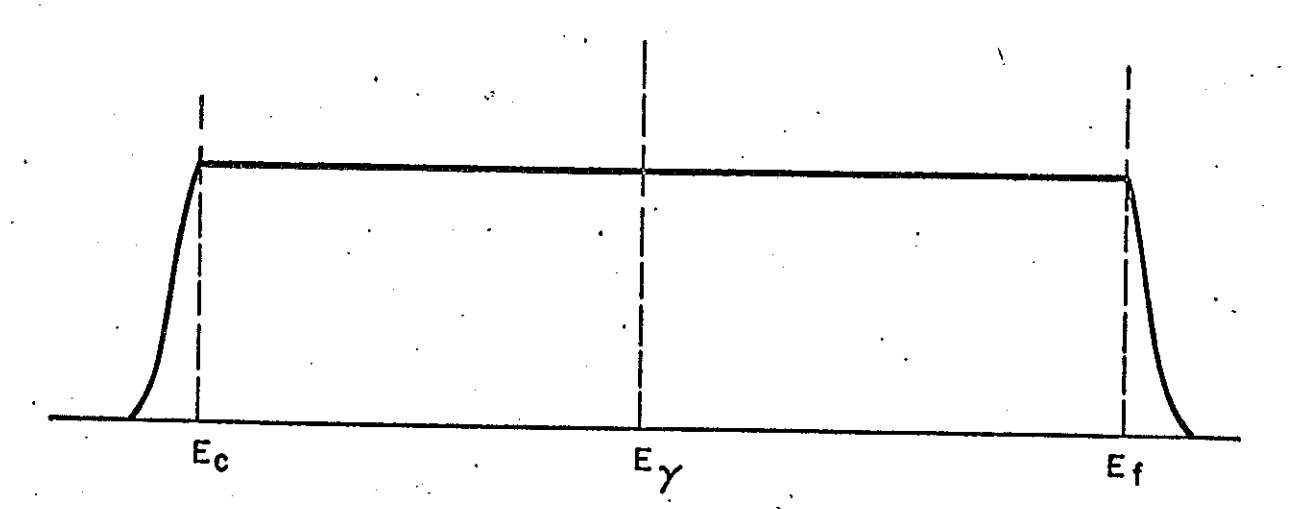
- Figure 1. Illustration of  $\gamma$ -ray Doppler shifts due to motion of the center-of-mass [(V/c)E $_{\gamma}$ ] and the motion of the product M $_4$  [ $\overline{v}_4$ /c)E $_{\gamma}$ ]. See text for explanation.
- Figure 2. Illustration of Doppler broadened  $\gamma$ -ray line shape for maximum isotropic broadening. See text for explanation.
- Figure 3. High energy  $\gamma$ -ray spectrum of the <sup>239</sup>Pu/Be neutron source in a water moderator obtained with a Ge(Li) detector. Shown are the full energy, single escape and double escape peaks of a) the 2223 keV  $\gamma$ -ray from thermal neutron capture in the hydrogen of the water, b) the 4439 keV Doppler broadened  $\gamma$ -ray from the <sup>9</sup>Be( $\alpha$ , $n\gamma$ ) <sup>12</sup>C reaction, and c) the 6129 keV  $\gamma$ -ray from inelastic neutron scattering from oxygen in the water.
- Figure 4. Gamma-ray detection resolution of  $30 \text{ cm}^3$  Ge(Li) detector as a function of energy.
- Figure 5. The line shapes of the full energy (4439 keV), single escape (4439-511 keV) and double escape (4439-1022 keV) peaks due to the Doppler broadened 4439 keV transition in the  ${}^9\text{Be}(\alpha,n\gamma){}^{12}\text{C}$  reaction. Obtained from the  ${}^{239}\text{Pu/Be}$  neutron source with the Ge(Li) detector.

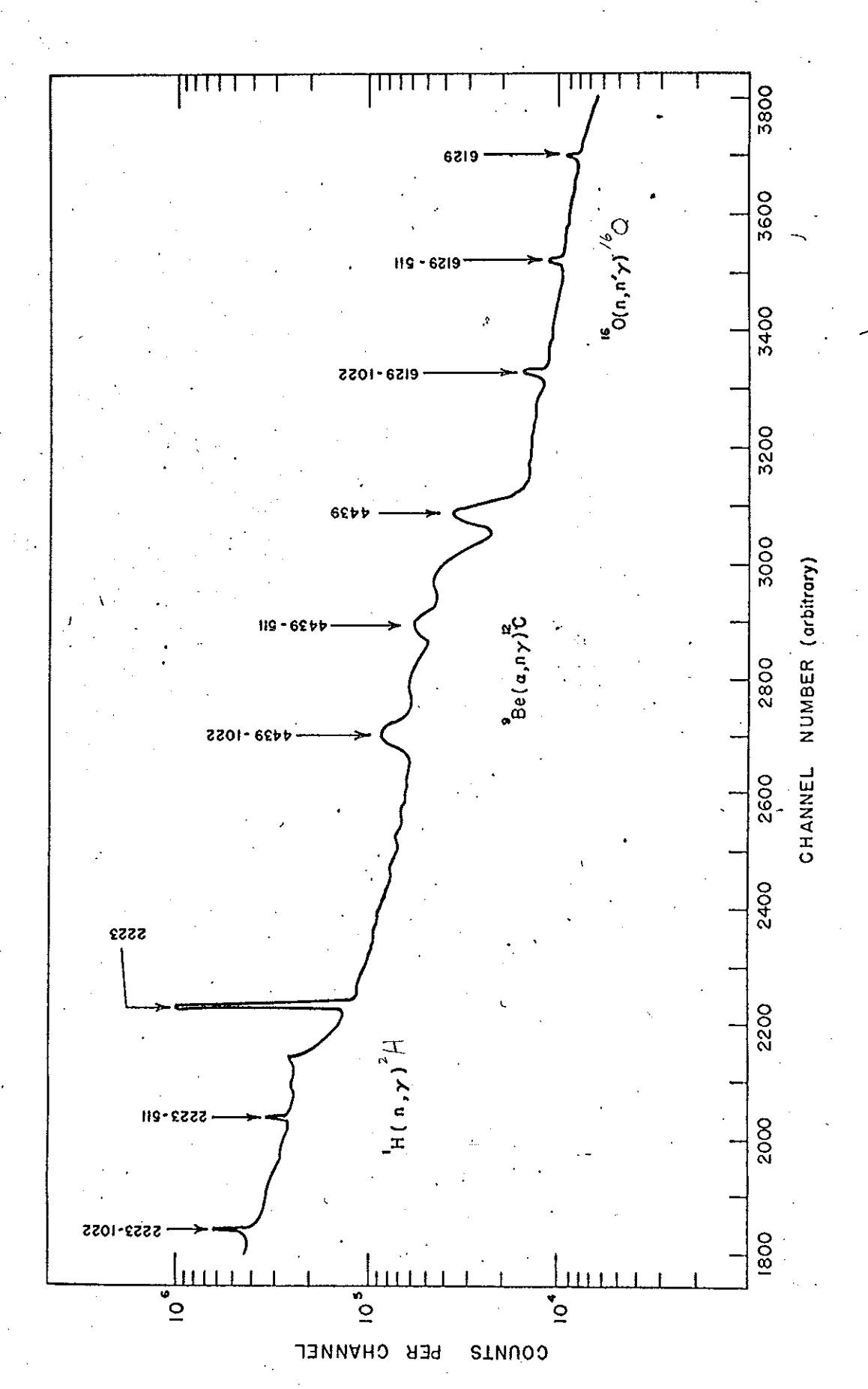


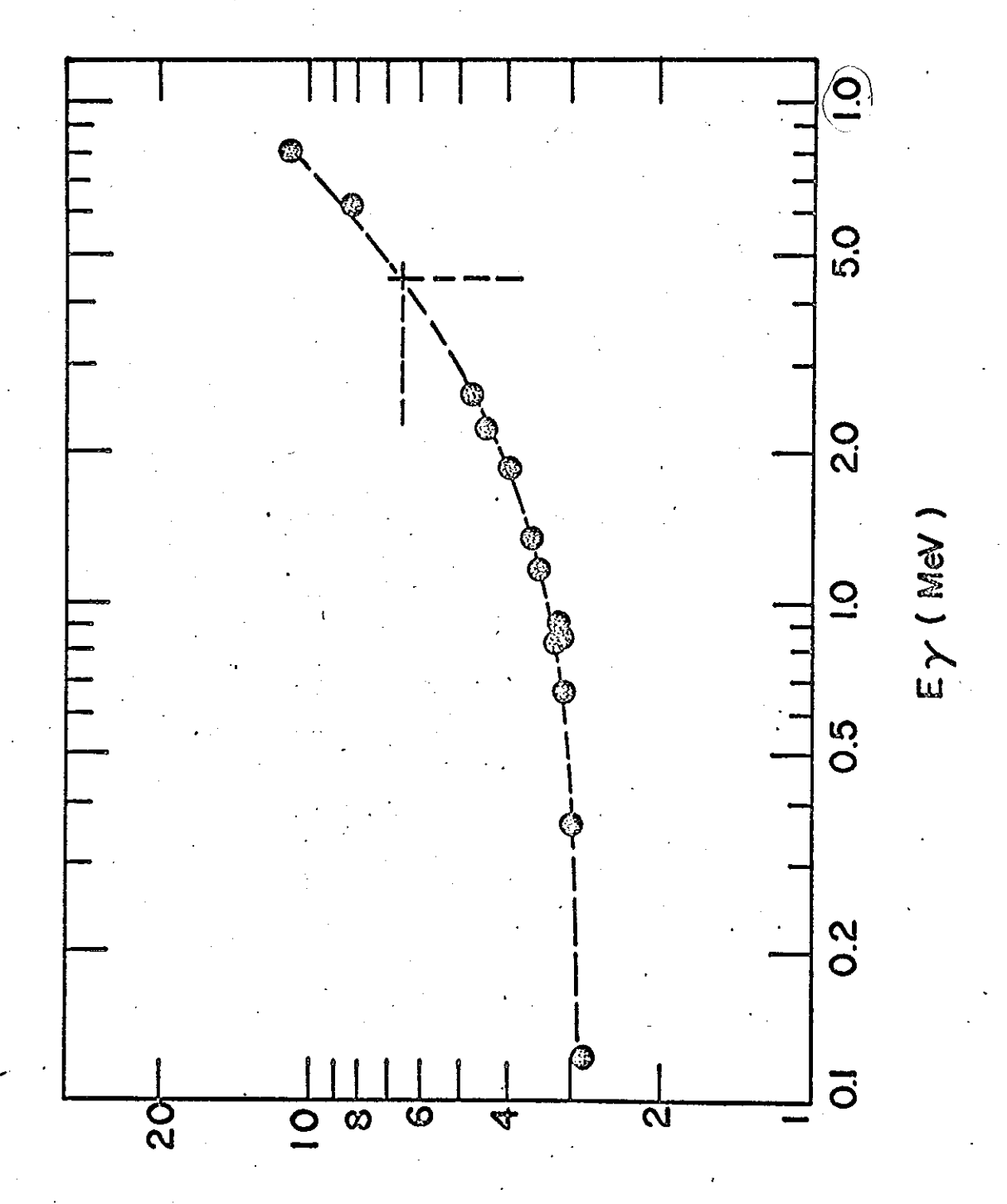












EMHW (KOA)